

# Noise sensitivity of an atomic velocity sensor

## Theoretical and experimental treatment

Pierre Cladé<sup>1</sup>, Saïda Guellati-Khélifa<sup>2</sup>, Catherine Schwob<sup>1</sup>, François Nez<sup>1</sup>, Lucile Julien<sup>1</sup> and François Biraben<sup>1</sup>

<sup>1</sup> Laboratoire Kastler Brossel, École Normale Supérieure, CNRS, UPMC, 4 place Jussieu, 75252 Paris Cedex 05, France

<sup>2</sup> CNAM-INM, Conservatoire National des Arts et Métiers, 292 rue Saint Martin, 75141 Paris Cedex 03, France

Received: date / Revised version: date

**Abstract.** We use Bloch oscillations to accelerate coherently Rubidium atoms. The variation of the velocity induced by this acceleration is an integer number times the recoil velocity due to the absorption of one photon. The measurement of the velocity variation is achieved using two velocity selective Raman  $\pi$ -pulses: the first pulse transfers atoms from the hyperfine state  $5S_{1/2}, |F=2, m_F=0\rangle$  to  $5S_{1/2}, |F=1, m_F=0\rangle$  into a narrow velocity class. After the acceleration of this selected atomic slice, we apply the second Raman pulse to bring the resonant atoms back to the initial state  $5S_{1/2}, |F=2, m_F=0\rangle$ . The populations in ( $F=1$  and  $F=2$ ) are measured separately by using a one-dimensional time-of-flight technique. To plot the final velocity distribution we repeat this procedure by scanning the Raman beam frequency of the second pulse. This two  $\pi$ -pulses system constitutes then a velocity sensor. Any noise in the relative phase shift of the Raman beams induces an error in the measured velocity. In this paper we present a theoretical and an experimental analysis of this velocity sensor, which take into account the phase fluctuations during the Raman pulses.

**PACS.** PACS-32.80.Pj Optical cooling of atoms; trapping – PACS-06.30.Gv Velocity, acceleration and rotation

## 1 Introduction

The measurement of the recoil of an atom when it absorbs a photon provides a way to determine the fine structure constant  $\alpha$  using atomic physics [1,2,3,4]. Since the first observation of the recoil-induced spectral doubling in the  $CH_4$  saturated absorption peaks [5], only the development of atoms cooling techniques renewed interest in measurement of the recoil velocity  $v_r$  ( $v_r = \hbar k/m$ , where  $k$  is the wave vector of the photon absorbed by an atom of mass  $m$ ) [2,3,4]. The basic scheme of the photon recoil, was previously proposed in reference [6] and a simple version is illustrated in Fig.1: an atom in state  $|a\rangle$ , at rest in the laboratory frame, absorbs a photon from rightward propagating laser beam with frequency  $\omega$ . The atom recoils by  $\hbar k/m$  and the process has the resonance condition deduced from energy conservation

$$\omega_{ab} - \omega = \frac{\hbar k^2}{2m} \quad (1)$$

The atom can be also de-excited from state  $|b\rangle$  by a photon from a leftward propagating beam of frequency  $\omega'$ , the new resonance condition being

$$\omega_{ab} - \omega' = -\frac{\hbar \vec{k} \cdot \vec{k}'}{m} - \frac{\hbar k'^2}{2m} \quad (2)$$

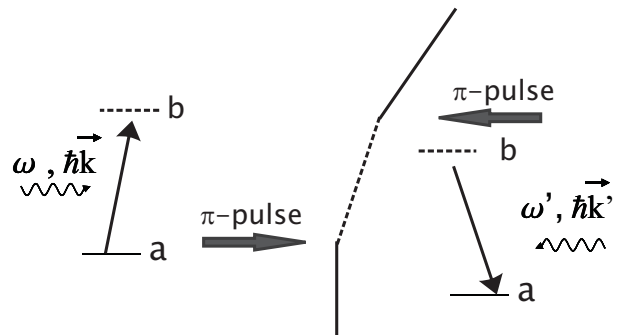


**Fig. 1.** Basic way to measure the photon recoil: the atom jumps from  $|a\rangle$  to  $|b\rangle$  by absorbing a rightward photon and acquires one recoil, and then it goes back into  $|a\rangle$  by re-emitting a leftward photon.

Thus, the two resonances are shifted relative to each other by

$$\omega - \omega' = -\frac{\hbar(\vec{k} + \vec{k}')^2}{2m} \quad (3)$$

If we fix  $\omega$  and scan  $\omega'$  to find the maximum number of atoms that come back to state  $|a\rangle$ , we can measure this frequency difference and hence deduce the recoil shift. The ideal recoil measurement described above will be more re-

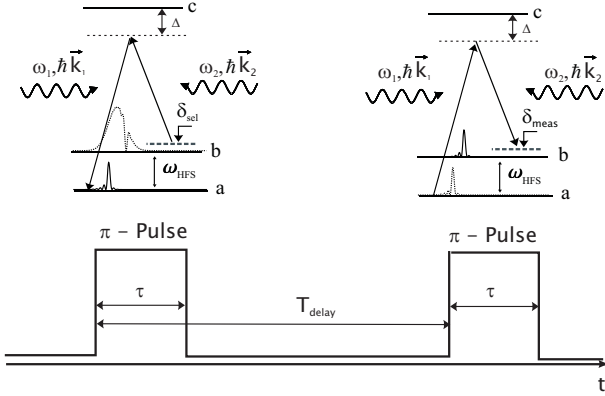


**Fig. 2.** Principle of the velocity sensor, the first  $\pi$ -pulse transfers a narrow velocity class from the level  $|b\rangle$  to the level  $|a\rangle$  (selection) and the second  $\pi$ -pulse transfers the accelerated atoms back to the level  $|b\rangle$  (measurement).

alistic using velocity-selective Raman transitions [7]. Transitions of this kind have two relevant advantages: first the effective frequency is the hyperfine splitting which is a microwave frequency and the effective momentum kick is equal to that obtained with optical photons (large Doppler shift). Second, as these transitions involve ground state atomic levels, the linewidth of the stimulated transition, and thus the width of the velocity distribution, is limited only by the interaction time which is quite long when cold atoms are used.

Let us consider an atomic cold sample where, after a laser cooling process, the atoms, all in a well defined internal state  $|b\rangle$ , are illuminated successively by two velocity-selective Raman  $\pi$ -pulses. The Raman excitation is realized by two counter-propagating laser beams at frequencies  $\omega_1$  and  $\omega_2$ , and wave vectors  $\vec{k}_1$  and  $\vec{k}_2$ . When the resonance condition:

$$\delta_{sel} = \omega_2 - \omega_1 - \omega_{HFS} = \vec{v}_i \cdot (\vec{k}_1 - \vec{k}_2) + \frac{\hbar(\vec{k}_1 - \vec{k}_2)^2}{2m} \quad (4)$$

is fulfilled, the first  $\pi$ -pulse transfers the atoms, in narrow velocity class around the mean velocity  $v_i$ , from state  $|b\rangle$  to  $|a\rangle$  (see Fig.2). Here  $\delta_{sel}$  is the detuning of the co-propagating Raman transition.

After an acceleration which changes the mean velocity of the atomic velocity class from  $v_i$  to  $v_f$ , we apply a second  $\pi$ -pulse and we shift the detuning to  $\delta_{meas}$  so as we satisfy the resonance condition (equation (4)) for the mean velocity  $v_f$ . By scanning the detuning  $\delta_{meas}$  of the final Raman pulse to get maximum of atoms back into initial state  $|b\rangle$ , we determine the variation of velocity  $\Delta \vec{v}$  by

$$\Delta \vec{v} \cdot (\vec{k}_1 - \vec{k}_2) = (\delta_{meas}^{max} - \delta_{sel}) \quad (5)$$

This system constitutes a velocity sensor. In our experiment the atoms are coherently accelerated using Bloch oscillations in a periodic optical potential [4, 10, 11]. In this case, the velocity variation of the center of mass is an integer times the recoil velocity  $v_r$ . In this paper we shall

ignore this intermediate step and only focus on the study of the velocity sensor described above. In the following we investigate theoretically the number of atoms in the state  $|b\rangle$  after the second  $\pi$ -pulse, starting by the determination of the Raman transition probability and taking into account the relative phase noise between the two counter-propagating beams. We then calculate the noise sensitivity of the velocity sensor and the ordinary variance of the measured atoms. Finally, we present the experimental set-up and discuss how the experimental compares with our theoretical model. We underline that previously other groups have studied the phase fluctuations of the Raman beams in atom interferometers [8, 9]. The originality of this work is to take into account the effects of the phase fluctuations during the Raman pulses and not only between the pulses.

## 2 Theory

The theory of velocity-selective stimulated Raman transitions was been widely studied by [7, 12]. In the subsection 2.1, we investigate the stimulated Raman transition probability considering the relative phase noise  $\varphi(t)$  (time dependence) between the two beams. In subsection 2.2, we consider the double  $\pi$ -pulse and we determine the fraction of atoms at a given detuning  $\delta$  of the Raman beam frequency. We then deduce the sensitivity of the velocity sensor by expressing the ordinary variance as function of a power spectral density of the phase noise.

### 2.1 One pulse Raman transition

We consider an atom that has a level scheme shown in Fig.2. with a ground state hyperfine interval  $\omega_{HFS}$ . This atom is irradiated, along the  $z$  axis, by two counter-propagating laser beams ( $\omega_1, \vec{k}_1$ ) and ( $\omega_2, \vec{k}_2$ ).

The states  $|a, p - \hbar k_1\rangle$  and  $|b, p + \hbar k_2\rangle$  are coupled to  $|c, p\rangle$  respectively by the wave ( $\omega_1, \vec{k}_1$ ) and ( $\omega_2, \vec{k}_2$ ). The atomic system is then equivalent to a two-level system coupled by a two-photon transition with an effective Rabi frequency :

$$\Omega = \frac{\Omega_1^* \Omega_2}{2\Delta} \quad (6)$$

where  $\Delta = \omega_1 - \omega_{ac} \approx \omega_2 - \omega_{bc}$  is the one photon detuning (see Fig.2) and the Rabi frequencies  $\Omega_1$  and  $\Omega_2$  are defined by

$$\Omega_1 = -\frac{\langle a | \vec{d} \cdot \vec{E}_1 | c \rangle}{2\hbar}, \Omega_2 = -\frac{\langle b | \vec{d} \cdot \vec{E}_2 | c \rangle}{2\hbar} \quad (7)$$

$\vec{E}_n$ , ( $n = 1, 2$ ) is the electric field of the travelling wave  $n$ ,  $\vec{d}$  is the electric dipole operator.

To include the relative phase noise  $\varphi(t)$  between the two Raman beams, we express the effective Rabi frequency as

$$\Omega(t) = \Omega_0 e^{i\varphi(t)} \quad (8)$$

Assuming that  $\varphi(t) \ll 1$ , the Hamiltonian of this two-level system can be linearized as the sum of  $H_0$  and  $H_{pert}$ , where in convenient Pauli matrix representation

$$H_0 = \hbar \left( \frac{\delta}{2} \sigma_z + \frac{\Omega_0}{2} \sigma_x \right) \quad (9)$$

$\delta$  is the detuning of  $\omega_1 - \omega_2$  from the transition  $|a, p - \hbar k_1\rangle \rightarrow |b, p + \hbar k_2\rangle$ .

The time dependent perturbative hamiltonian in first order approximation is given by

$$H_{pert}(t) = i\hbar \frac{\Omega_0}{2} \varphi(t) \sigma_x \quad (10)$$

The state of a quantum system at a final time  $t_f$  is related to its state at an earlier time  $t_i$  via the evolution operator  $U$

$$|\psi(t_f)\rangle = U(t_f, t_i) |\psi(t_i)\rangle \quad (11)$$

using the time dependent perturbation theory, in first order, the evolution operator  $U$  is given by

$$U(t_f - t_i) = U_0(t_f - t_i) + \frac{1}{i\hbar} \int_{t_i}^{t_f} U_0(t_f - t) H_{pert}(t) U_0(t - t_i) dt \quad (12)$$

where

$$U_0(t) = e^{-i \frac{H_0 t}{\hbar}} \quad (13)$$

The time dependent transition probability  $P$  from level  $|a\rangle$  to level  $|b\rangle$  is

$$P(\delta) = |\langle a|U|b\rangle|^2 \quad (14)$$

Substituting the relations (12) and (13) into equation (14) we show that the transition probability can be written as

$$P(\delta) = P^0(\delta) + P^1(\delta) \quad (15)$$

$P^0$  is given by the Rabi formula:

$$P^0(\delta) = \frac{\Omega_0^2}{\Omega'^2} \sin^2 \frac{\Omega'(t_f - t_i)}{2} \quad (16)$$

and  $P^1$ , the time dependent transition probability to first order in the relative phase noise is given by

$$P^1(\delta) = -\delta \frac{\Omega_0^2}{\Omega'^2} \sin \frac{\Omega'(t_f - t_i)}{2} \int_{t_i}^{t_f} \varphi(t) \sin \frac{\Omega'(2t - t_f - t_i)}{2} dt \quad (17)$$

where

$$\Omega' = \sqrt{\Omega_0^2 + \delta^2} \quad (18)$$

is the generalized Rabi frequency.

## 2.2 Selection and Measurement

We consider now an atom in internal state  $|b\rangle$  with an initial velocity  $v_i$  along the beams axis. This atom is illuminated consecutively by two Raman  $\pi$ -pulses with the same duration  $\tau$  and separated by the time interval  $T_{delay}$  (see Fig.2). During the time interval between the two  $\pi$ -pulses, the atom is accelerated to change its velocity by  $\Delta v$  (the final velocity is then  $v_f = v_i + \Delta v$ ).  $P_{sel}(\delta_{sel} - 2kv_i)$  and  $P_{meas}(\delta_{meas} - 2kv_f)$  are respectively the probability to make the first and the second Raman transition.

The experimental proceeding of the velocity sensor was described in the first section and illustrated in the Fig.2. The atoms remaining in level  $|b\rangle$  after the first  $\pi$ -pulse, are pushed away using a resonant laser beam. The distribution velocity of the selected velocity class is supposed constant along the width of the selection ( $n(v) = n_0$ ) (in fact, the typical width of the initial distribution obtained with an optical molasses in a few recoils, whereas the first  $\pi$ -pulse selects atoms in a velocity class of about  $v_r/30$ ). After the second pulse, we measure separately the number of atoms in state  $|a\rangle$  and  $|b\rangle$  using two parallel, horizontally propagating probe beams, placed 15 cm below the center of the trap and separated vertically by 1 cm. The number  $N_b$  of atoms transferred by the second pulse is equal to the contribution of all selected atoms weighted by the probability to make the second  $\pi$ -pulse Raman transition:

$$N_b(\delta_{meas} - \delta_{sel}) = \frac{n_0}{2k} \int_{-\infty}^{+\infty} P_{sel}(\delta_{sel} + \eta) P_{meas}(\delta_{meas} - 2k\Delta v + \eta) d\eta \quad (19)$$

where  $\eta = -2kv_i$ .

The total number  $N_a + N_b$  of atoms detected after the second pulse is nothing more than the number  $N_{sel}$  of atoms selected by the first  $\pi$ -pulse:

$$N_{sel}(\delta_{sel}) = n_0 \int_{-\infty}^{\infty} P_{sel}(\delta_{sel} - 2kv_i) dv_i \quad (20)$$

To eliminate the fluctuations of the initial number of atoms, we consider in the following the probability  $\mathcal{P} = N_b/(N_a + N_b)$  which represents the velocity distribution of the measured atomic fraction. By inserting (15) in (19) and using the fact that  $P^1$  is an even function, we finally obtain the correction of  $\mathcal{P}$  to first order in  $\varphi(t)$ :

$$\mathcal{P}^1(\delta + 2k\Delta v) = \frac{\int_{-\infty}^{+\infty} P^0(\eta - \delta) (P_{sel}^1(\eta) - P_{meas}^1(\eta)) d\eta}{\int_{-\infty}^{\infty} P^0(\eta) d\eta} \quad (21)$$

where in thus case  $\delta$  is equal to  $\delta_{meas} - 2k\Delta v - \delta_{sel}$ .

## 2.3 Determination of the transfer function $H(f, \delta)$

The best way to test the propagation of the phase fluctuation  $\varphi(t)$  on the velocity sensor is to calculate the ordinary

variance  $\sigma_{\mathcal{P}}$  of the probability  $\mathcal{P}$  to make the two Raman transitions.

$$\sigma_{\mathcal{P}}^2(\delta) = \langle (\mathcal{P} - \langle \mathcal{P} \rangle)^2 \rangle \quad (22)$$

The probability  $\mathcal{P}$  is a linear function of  $\varphi(t)$  (inserting (17) in (21)). Assuming that  $\varphi$  is a stationary random variable, we can express  $\sigma_{\mathcal{P}}$  as a function of the density of the noise  $\Phi_f$

$$\sigma_{\mathcal{P}}^2(\delta) = \int_{-\infty}^{+\infty} \Phi_f^2 H^2(f, \delta) df \quad (23)$$

where

$$\Phi_f^2 = 4 \int_{-\infty}^{+\infty} d\tau e^{2\pi i f \tau} \langle \varphi(t + \tau) \varphi(t) \rangle \quad (24)$$

and  $H(f, \delta)$  represents the transfer function or the noise sensitivity of the velocity sensor. To easily calculate this last function using (21), we will assume that the phase fluctuation between the Raman beams can be expressed as

$$\varphi(t) = \sum_f \Phi_f \sqrt{\Delta f} \cos(2\pi f t + \varphi_f) \quad (25)$$

where  $\varphi_f$  are arbitrary phases at each frequency  $f$  (we assume that the phases  $\varphi_f$  between two different frequencies are independent). At the limit where the frequency band  $\Delta f \rightarrow 0$ , the two points of view in equations (24) and (25) give the same result for  $H(f, \delta)$ . In equation (25) the noise density  $\Phi_f$  is expressed in ( $rad/\sqrt{Hz}$ ).

First we calculate the one  $\pi$ -pulse transition using the expression of  $\varphi(t)$  (25) in (17):

$$P^1(\delta) = -\delta \frac{\Omega_0^2}{\Omega'^2} \sin \frac{\Omega'}{2} (t_f - t_i) \sum_f \Phi_f \sin(\pi f (t_f + t_i) + \varphi_f) \left( \frac{\sin((2\pi f + \Omega') \frac{(t_f - t_i)}{2})}{2\pi f + \Omega'} - \frac{\sin((2\pi f - \Omega') \frac{(t_f - t_i)}{2})}{2\pi f - \Omega'} \right) \sqrt{\Delta f} \quad (26)$$

Second we calculate the two Raman transitions probability (for two  $\pi$ -pulses) substituting  $P^1$  by (26) in (21)

$$P^1(\delta + 2k\Delta v) = \sum_f \Phi_f h(f, \delta) \cos(\pi f (T_{delay} + \tau) + \varphi_f) \sqrt{\Delta f} \quad (27)$$

where

$$h(f, \delta) = \int_{-\infty}^{+\infty} 2P_0(\eta - \delta) \delta \frac{\Omega_0^2}{\Omega'^2} \sin \frac{\Omega'}{2} \sin(\pi f T_{delay}) \left( \frac{\sin(2\pi f - \Omega') \frac{\tau}{2}}{2\pi f - \Omega'} - \frac{\sin(2\pi f + \Omega') \frac{\tau}{2}}{2\pi f + \Omega'} \right) d\eta \quad (28)$$

with  $\tau = t_f - t_i$  and  $T_{delay}$  is the time interval between the two  $\pi$ -pulses. To simplify the presentation of the formula (28) the normalization factor in (21) is omitted.

Since for each frequency,  $\varphi_f$  is a random variable with an uniform distribution on  $[0, 2\pi]$ , then

$$\langle \mathcal{P}^1 \rangle = 0 \quad \text{and} \quad \langle (\mathcal{P}^1)^2 \rangle = \sum_f \frac{1}{2} \Phi_f^2 h^2(f, \delta) \Delta f \quad (29)$$

Substituting (29) in the definition of the ordinary variance  $\sigma_{\mathcal{P}}$ , we deduce the expression of the transfer function  $H(f, \delta)$

$$H(f, \delta) = \frac{1}{\sqrt{2}} |h(f, \delta)| \quad (30)$$

This function depends on the pulse interval on  $\sin(\pi f T_{delay})$  (see (28)): for each  $T_{delay}$  there are certain frequencies at which the phase noise does not have any effect.

### 3 Experiment

An optical molasses loaded by a 3-D magneto-optical trap provides a cold  $^{87}Rb$  atomic sample [4]. For the initial selection and the final measurement, the two Raman beams are generated by two laser diodes injected by two grating-stabilized extended-cavity laser diodes (ECLs). A fast photodiode and a tunable RF frequency chain are used to phase lock one ECL on the other one. The two beams have linear orthogonal polarizations. After passing through the vacuum cell, one beam is retroreflected by a horizontal mirror (see Fig.3). A typical scan of final velocity distribution of Rubidium atoms transferred by the second pulse from  $5S_{1/2} |F=1, m_F=0\rangle$  to  $5S_{1/2} |F=2, m_F=0\rangle$ , is shown in Fig. (4.b). The noise level affecting a measured spectrum is not uniform: it is lightly greater on the slopes than on the top. A better illustration of the noise distribution affecting the spectrum can be achieved by plotting the difference between the theoretical fit and the experimental data (Fig.4). Thus is a proof that the spectral noise is not yet dominated by the atomic shot noise (number of detected atoms) but by the Raman phase noise. This phase noise can arise from optical noise (laser noise, fiber noise, phase lock noise, ...) or the vibration noise of the retroreflection mirror (indeed, the velocity of the atoms is measured in the frame of this mirror).

The resolution of our velocity sensor is then mainly limited by the Raman phase noise. In the next section we analyze the experimental results using the theoretical model developed above considering only the vibrational noise affecting the retroreflection mirror.

### 4 Analysis of the experimental results

The Raman beam phase noise includes different noise sources, it can be written essentially as a sum of two contributions:

$$\varphi(t) = [\varphi_1(t) - \varphi_2(t)] - 2k_2 x(t) \quad (31)$$

where  $\varphi_i(t)$  is the optical phase of the beam  $i$ ,  $x(t)$  characterizes the motion of the retroreflection mirror.

A straightforward way to distinguish between the vibration noise and other phase noises, is to compare the

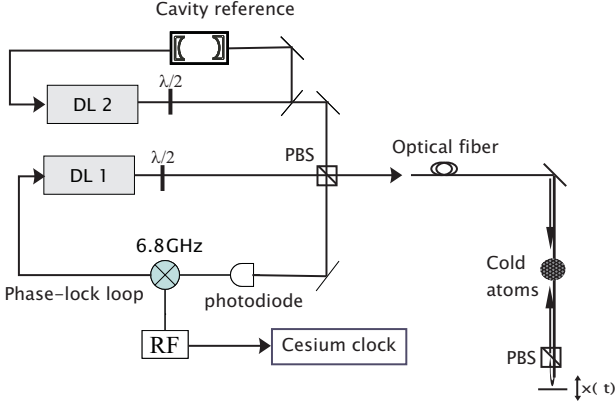


**Fig. 3.** Experimental setup of the velocity sensor: The two laser diodes are phase locked using a tunable microwave chain. The two Raman beams with  $\text{lin} \perp \text{lin}$  polarizations are injected into the same optical fiber. After passing through the vacuum chamber only the beam  $k_2$  is retroreflected by the horizontal mirror allowing a counter-propagating excitation.

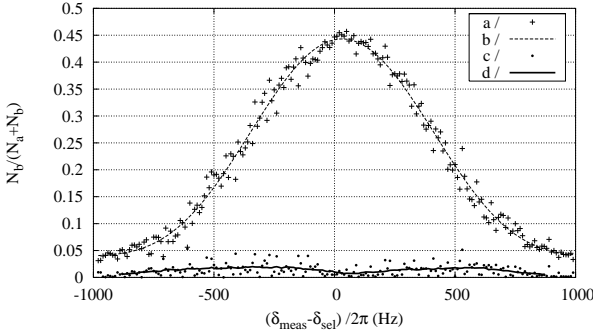


**Fig. 4.** a) Final velocity distribution of atoms in hyperfine state  $|F = 2, m_F = 0\rangle$  measured using two counter-propagating Raman beams and normalized to  $N_{sel} = N_a + N_b$  the number of atoms selected by the first pulse ( $N_a$  and  $N_b$  are successively the number of atoms measured in the hyperfine states  $|F = 1, m_F = 0\rangle$  and  $|F = 2, m_F = 0\rangle$ ). b) Theoretical fit. c) Difference between the experimental data and the theoretical fit. d) Smoothing curve of the last data using a fixed window. We note finally that in x-axis the velocity is expressed in terms of frequency.

Doppler-insensitive Raman transition spectrum obtained using a co-propagating beams (unaffected by vibrations of the retroreflection mirror) (Fig.5.a) to the Doppler-sensitive Raman transition spectrum driven by the counter-propagating laser beams (Fig.5.b).

This illustration shows that the relative noise is more than one order of magnitude lower in Fig.5 than in the case of the Doppler-sensitive Raman transition. Given thus, the optical phase noise  $\varphi_1(t) - \varphi_2(t)$  is not a relevant noise in our experimental set-up. In order to test the theoretical model presented above, we only take into account in expression (31) the vibration term. The phase noise spectral density can be expressed [13] as

$$\Phi_f = \frac{2k}{(2\pi f)^2} \Phi_f^a \quad (32)$$

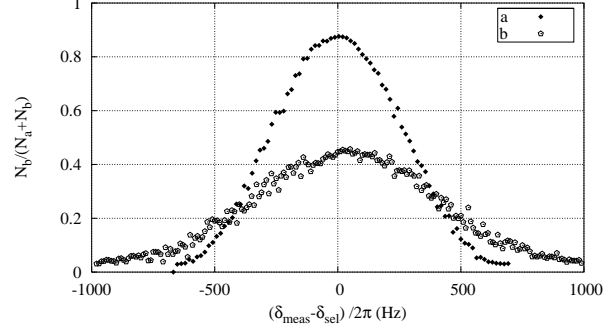


**Fig. 5.** The fraction of atoms transferred by the second Raman  $\pi$ -pulse: a) Co-propagating Raman beams configuration, b) Counter-propagating configuration. In this last case, the Doppler-sensitive Raman transition is performed only for a resonant velocity class. This explain the amplitude and the FWHM difference between the two spectra.

where  $\Phi_f^a$  is the acceleration noise spectral density, deduced from the acceleration of the mirror which is measured by a low-noise, low-frequency accelerometer (IMI Sensors-626A). The Fig.6.a, shows the acceleration noise power spectrum ( $\Phi_f^a$ ) of the retroreflection mirror. It is determined using a numerical Fourier transform of the monitored accelerometer signal. The rms value of the vibrational phase noise integrated on the pulse duration is estimated to  $0.1 \text{ rad}$ , and remains in the validity range of the perturbative approach used in our theoretical model.

The vibration sensitivity of the velocity sensor  $(2kH(f))/(2\pi f)^2$  is plotted for a pulse duration of 1 ms and a time spacing pulse  $T_{delay}$  of 12 ms using the (Fig.6.b). This curve shows that the velocity sensor acts as a low-pass filter of vibrations, with a cut off frequency of about 35 Hz. The effect of the mechanical vibration on the uncertainty of the velocity measurement can be illustrated by plotting a predicted variance  $\sigma_P$  using the acceleration noise spectral density (Fig.6.a) and the vibration sensitivity (Fig.6.b). It appears that the main part of the vibration noise in our experimental set-up comes from frequencies between 10 and 30 Hz (Fig.6.c).

As predicted by the theoretical model and illustrated in the typical velocity distribution spectrum (Fig.4), the noise of the velocity sensor depends on the Raman detuning  $\delta$ . By making several measurements at the same detuning  $\delta$ , we measure the statistical variance  $\sigma_P$  of the transition probability of the two Raman pulses (Fig.7).

The good qualitative and quantitative agreements with the predicted variance, allow us to confirm that the theoretical model developed in this paper is a powerful tool for quantifying and hence controlling the different noises of the Raman beams.

The time interval  $T_{delay}$  is a critical parameter of the experiment, it determines the number of additional recoils transferred by the Bloch oscillations process and hence the resolution of the photon recoil measurement. It will be useful to understand how this parameter operates on the uncertainty. In the Fig.8, the dots present the uncertainty on the measured velocity in term of frequency. This

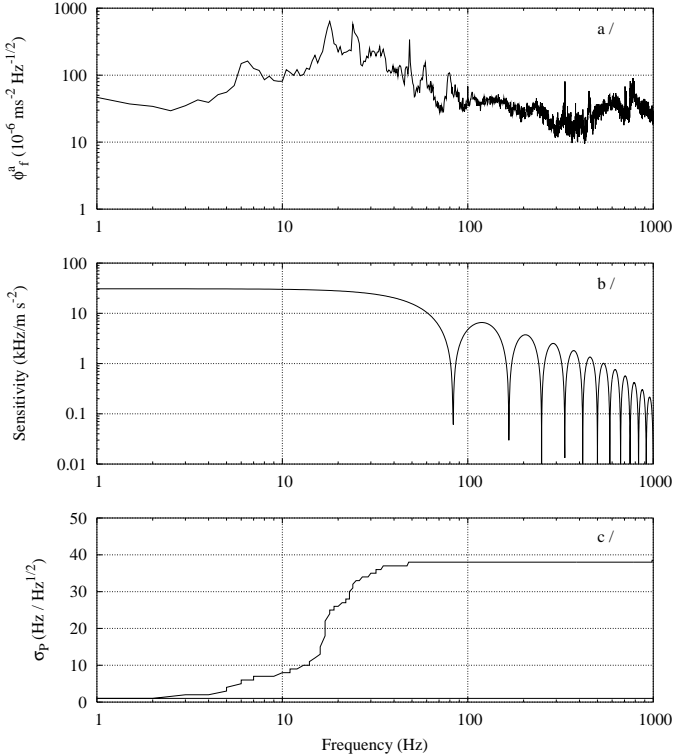


**Fig. 6.** (a). The acceleration noise spectral density deduced from the vibrational spectrum of the retroreflection mirror measured by an accelerometer. (b) The theoretical velocity sensor noise sensitivity for pulse duration  $\tau=1$  ms and pulse interval  $T_{delay}=12$  ms. (c) Predicted variance of the atoms fraction transferred by the second pulse integrated up to a certain frequency calculated using in the formula (23) the measured phase noise spectral density.

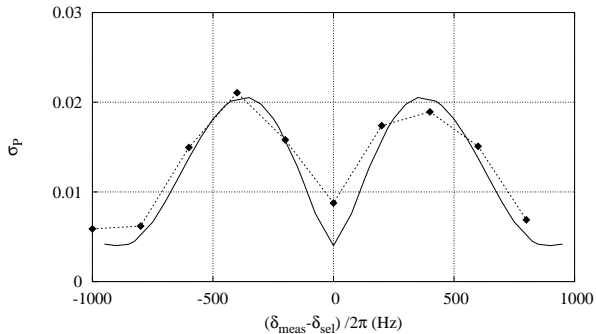


**Fig. 7.** Variance on the fraction of atoms transferred by the second  $\pi$ -pulse, dashed line experimental result, solid line predicted value.

uncertainty is deduced from the least-square fit of the experimental data points of the final velocity distribution by the non-perturbative part of the two pulses transition probability  $\mathcal{P}^0$ . We remind that this probability is determined substituting in (19)  $P_{sel}$  and  $P_{meas}$  by the one pulse Raman non-perturbative transition probability  $P^0$

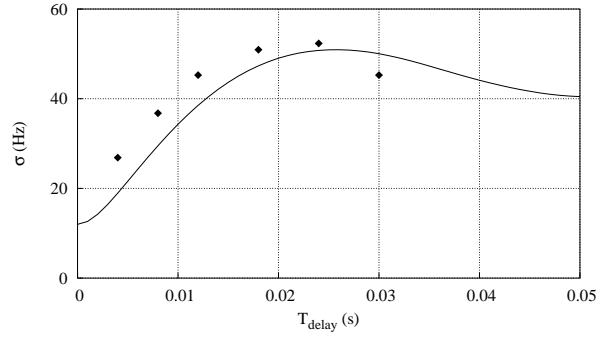


**Fig. 8.** The uncertainty of the measured velocity expressed in term of frequency, for different  $T_{delay}$ , predicted value (line) and experimental value (dot).

defined in (16). To predict this uncertainty, denoted  $\sigma$ , using the previous model we use the following formula

$$\sigma^2 = \frac{1}{n} \frac{\sum_{\delta} \sigma_{\mathcal{P}}^2}{\sum_{\delta} (\frac{\partial \mathcal{P}^0}{\partial \delta})^2} \quad (33)$$

where  $n$  is the number of the sample. This expression is obtained by substituting in the expression of the uncertainty given by a least square fit algorithm, the deviation of the numerical data from the theoretical function, by the theoretical mean uncertainty  $\sigma_{\mathcal{P}}$ . In this plot the noise increases with  $T_{delay}$  and reaches a maximum value, the noise decreases then, because the band pass of the velocity sensor varies as  $1/T_{delay}$  and then it filters the high vibrational noise frequencies.

## 5 Conclusion

In this paper we have developed a simple theoretical tool, to characterize the noise of an atomic velocity sensor. We have focused on the phase fluctuations of the Raman beams during the pulse, such effects are very important in our non-interferometric velocity sensor where the resolution is inversely proportional to the Raman pulses duration. The experimental illustration was here limited to the vibrational noise, but the model can be used for any other phase noise at the limit of the validity of the perturbative approach. This tool allows us to understand how to implement the experimental improvements, essentially the vibration isolation.

We thank A. Clairon and co-workers for valuable discussions. This experiment is supported in part by the Bureau National de Métrologie (Contrats 993009 and 033006) and by the Région Ile de France (Contrat SESAME E1220).

## References

1. B.N. Taylor, *Metrologia*. **31**, 181 (1994).
2. A. Wicht, J.M. Hensley, E. Sarajlic and S. Chu, *Proceedings of the 6th Symposium on Frequency Standards and Metrology*, eds. P. Gill (World Scientific, Singapore), pp 193-212 (2001).

3. S. Gupta, K. Dieckmann, Z. Hadzibabic and D.E. Pritchard, *Phys. Rev. Lett.* **89**, 140401-1 (2002).
4. R. Battesti, P. Cladé, S. Guellati-Khélifa, C. Schwob, B. Grémaud, F. Nez, L. Julien and F. Biraben, *Phys. Rev. Lett.* **92**, 253001-1 (2004).
5. J.L. Hall, C.J. Bordé and K. Uehara, *Phys. Rev. Lett.* **37**, 1339 (1976).
6. D.S. Weiss, B.C. Young and S. Chu *Appl.Phys.B*, **59**, 217-256 (1994).
7. M. Kasevich, D.S. Weiss, E. Riis, K. Moler, S. Kasapi and S. Chu, *Phys. Rev. Lett.* **66**, 2297 (1991).
8. A. Peters, K.Y. Chung and S. Chu *Metrologia* **38**, 25 (2001).
9. F. Yver-Leduc, P. Cheinet, J. Fils, A. Clairon, N. Dimarq, D. Holleville, P. Bouyer and A. Landragin *J. Opt. B.: Quantum Semiclassical* **5**, S136-S142 (2003).
10. M. Ben Dahan, E. Peik, J. Reichel, Y. Castin and C. Salomon, *Phys. Rev. Lett.* **76**, 4508 (1996).
11. E. Peik, M. Ben Dahan, I. Bouchoule, Y. Castin and C. Salomon, *Phys. Rev. A* **55**, 2989 (1997).
12. K. Moler, D.S. Weiss, M. Kasevich and S. Chu, *Phys. Rev A*. **45**, 342 (1992).
13. The phase noise induced by the vibration of the retroreflecting mirror is  $\varphi(t) = 2k_2x(t)$  then the acceleration of this mirror  $a(t)$  can be written as  $a(t) = \sum \frac{(2\pi f)^2 \Phi_f}{2k} \sqrt{\Delta f} \cos(2\pi ft + \varphi_f)$ .